Vilnius University
Faculty of Physics
Laboratory of Atomic and Nuclear Physics

Experiment No. 11

# STUDY OF THE ALPHA-ENERGIES OF RADIUM-226

by Andrius Poškus
(e-mail: andrius.poskus@ff.vu.lt)

2025-04-08

**Contents**

# The aim of the experiment

Measure alpha particle energy distribution with a semiconductor spectrometer; test some properties of alpha energy spectrum (discrete character of alpha particle spectrum, typical energies of alpha particles emitted by radioactive nuclides, proportionality of detector pulse height to energy of incident particle), investigate influence of interaction of alpha particles with matter on the shape of their energy spectrum.

# 1. Tasks

1. Measure energy spectrum of alpha particles emitted by a sealed source containing the isotope of radium $^{226}$Ra, which is in radioactive equilibrium with its decay products.
2. Measure the calibration spectrum using an unsealed source containing the isotope of americium $^{241}$Am, under the same conditions as in Task 1.
3. Calculate particle energies corresponding to the peaks of the $^{226}$Ra spectrum.
4. Calculate the differences of alpha particle energies corresponding to various pairs of peaks in the $^{226}$Ra spectrum.
5. Compare the obtained differences of energies with differences of true (initial) energies corresponding to various pairs of nuclides in the decay chain of $^{226}$Ra. Under the assumption that all alpha particles lose the same energy amount in the source cover, the measured energy differences should be equal to differences of corresponding initial energies. Based on this comparison, determine the nuclides corresponding each peak in the measured $^{226}$Ra spectrum.
6. Discuss the shape of the spectra (difference of peak widths in $^{241}$Am and $^{226}$Ra spectra, positions of peaks in the $^{226}$Ra spectrum, similarities and differences of peak integrals), explain the observed features of the spectra on the basis of the theory of alpha particle interaction with matter (i.e., with the cover of the $^{226}$Ra source) and the theory of radioactive equilibrium.

# 2. Control questions

1. What are the types of ionizing radiation?
2. Define the concept of radioactivity. Formulate the law of radioactive decay. Derive the expression of activity of a radioactive nuclide.
3. Define the concept of a decay chain. What is radioactive equilibrium? How are amounts of radioactive nuclides related to each other under conditions of radioactive equilibrium?
4. What is alpha decay? What are its main properties?
5. Formulate the Geiger-Nuttall law, explain it qualitatively.
6. What is the origin of energy losses of alpha particles in matter? Define the concept of energy straggling.
7. Explain the concept of detector pulse height spectrum and its relation to the particle energy spectrum. Define energy resolution of a detector.

**Recommended reading**:

1. Krane K. S. Introductory Nuclear Physics. New York: John Wiley & Sons, 1988. p. 160 – 165, 193 – 198, 246 – 254.
2. Lilley J. Nuclear Physics: Principles and Applications. New York: John Wiley & Sons, 2001. p. 14 – 15, 18 – 22, 84 – 88, 129 – 136.
3. Knoll G. F. Radiation Detection and Measurement. 3rd Edition. New York: John Wiley & Sons, 2000. p. 30 – 34.
4. Payne M. G. Energy straggling of heavy charged particles in thick absorbers // Physical Review, vol. 185, no. 2, 1969, p. 611 – 623.
5. Laboratory Experiments. Phywe Systeme GmbH, 2005 (*compact disc*).

# 3. The types of ionizing radiation

***Ionizing radiation*** is a flux of subatomic particles (e. g. photons, electrons, positrons, protons, neutrons, nuclei, etc.) that cause ionization of atoms of the medium through which the particles pass. ***Ionization*** means the removal of electrons from atoms of the medium. In order to remove an electron from an atom, a certain amount of energy must be transferred to the atom. According to the law of conservation of energy, this amount of energy is equal to the decrease of kinetic energy of the particle that causes ionization. Therefore, ionization becomes possible only when the energy of incident particles (or of the secondary particles that may appear as a result of interactions of incident particles with matter) exceeds a certain threshold value – the ***ionization energy*** of the atom. Ionization energies of isolated atoms are usually of the order of a few electronvolts (eV). 1 eV = $1{,}6022 \cdot 10^{-19}$ J. The ionization energies of molecules of most gases that are used in radiation detectors are between 10 eV and 25 eV.

Ionizing radiation may be of various nature. The ***directly ionizing radiation*** is composed of high-energy charged particles, which ionize atoms of the material due to Coulomb interaction with their electrons. Such particles are, e. g., high-energy electrons and positrons (beta radiation), high-energy $^4$He nuclei (alpha radiation), various other nuclei. ***Indirectly ionizing radiation*** is composed of neutral particles, which do not directly ionize atoms or do that very infrequently, but due to interactions of those particles with matter high-energy free charged particles are occasionally emitted. The latter particles directly ionize atoms of the medium. Examples of indirectly ionizing radiation are high-energy photons (ultraviolet, X-ray and gamma radiation) and neutrons of any energy. Particle energies of various types of ionizing radiation are given in the two tables below.

**Table 1**. The scale of wavelengths of electromagnetic radiation

| Spectral region | Approximate wavelength range | Approximate range of photon energies |
|---|---|---|
| Radio waves | 100000 km – 1 mm | $1 \cdot 10^{-14}$ eV – 0,001 eV |
| Infrared rays | 1 mm – 0,75 μm | 0,001 eV – 1,7 eV |
| Visible light | 0,75 μm – 0,4 μm | 1,7 eV – 3,1 eV |
| Ionizing electromagnetic radiation: | | |
| Ultraviolet light | 0,4 μm – 10 nm | 3,1 eV – 100 eV |
| X-ray radiation | 10 nm – 0,001 nm | 100 eV – 1 MeV |
| Gamma radiation | < 0,1 nm | > 10 keV |

**Table 2**. Particle energies corresponding to ionizing radiation composed of particles of matter

| Radiation type | Approximate range of particle energies |
|---|---|
| Alpha (α) particles ($^4$He nuclei) | 4 MeV – 9 MeV |
| Beta (β) particles (electrons and positrons) | 10 keV – 10 MeV |
| Thermal neutrons | < 0,4 eV |
| Intermediate neutrons | 0,4 eV – 200 keV |
| Fast neutrons | > 200 keV |
| Nuclear fragments and recoil nuclei | 1 MeV – 100 MeV |

The mechanism of interaction of particles with matter depends on the nature of the particles (especially on their mass and electric charge). According to the manner by which particles interact with matter, four distinct groups of particles can be defined:

1) heavy charged particles (such as alpha particles and nuclei),

2) light charged particles (such as electrons and positrons),

3) photons (neutral particles with zero rest mass),

4) neutrons (neutral heavy particles).

This experiment concerns only the first mentioned type of particles (heavy charged particles).

# 4. Radioactive decay

## 4.1. The concept of radioactive decay

In radioactive decay, an unstable nucleus (called "parent") is transformed into a more stable nuclide (called the "daughter"). If the daughter nuclide is also radioactive, the process continues in a ***decay chain*** until a stable nuclide is reached.

Radioactivity is a random process. We cannot know exactly when a given unstable nucleus will decay and can only specify a probability per unit time that it will do so. This probability is called the ***decay constant***. It is frequently denoted by the Greek letter $\lambda$. Another quantity, which is related to the decay constant, is the decay ***half-life*** ($t_{1/2}$). It is the time taken for half the nuclei in a sample to decay:

$$t_{1/2} = \frac{\ln 2}{\lambda} \tag{4.1.1}$$

The mean time until the decay of a nucleus is called its mean ***lifetime***:

$$\tau = \frac{1}{\lambda} \tag{4.1.2}$$

If a given radioactive nuclide is not created (i.e., it is not a daughter of another nuclide, and it is not created in any nuclear reaction), then its amount decreases exponentially with time:

$$N(t) = N(0)\exp(-\lambda t) \equiv N(0)2^{-t/t_{1/2}} \tag{4.1.3}$$

Decay rate $-\mathrm{d}N / \mathrm{d}t$ is called ***activity***. Unit of activity is becquerel (Bq): 1 Bq = 1 $\mathrm{s}^{-1}$. As evident from the previous equation,

$$\frac{\mathrm{d}N}{\mathrm{d}t} = -\lambda N(t) \tag{4.1.4}$$

I.e., activity of a given nuclide is equal to its decay constant times the current number of atoms of this nuclide. The equality (4.1.4) is the differential form of the radioactive decay law (expression (4.1.3) is the solution of the differential equation (4.1.4)).

All naturally occurring, and the majority of artificially produced, radioactive nuclei are either $\alpha$ active, $\beta$ active, or both, and emit a combination of $\alpha$, $\beta$ and $\gamma$ radiation. Artificially produced unstable nuclei may also decay by emitting protons, neutrons or even heavy ions.

## 4.2. Radioactive decay chains. Radioactive equilibrium

The daughter nucleus, which is formed due to decay of the parent nucleus, is frequently radioactive, too. Its decay product can also be radioactive, etc. Such a sequence of radioactive decays is called a ***decay chain***. Let us assume that the decay chain consists of decays $\mathrm{A} \rightarrow \mathrm{B} \rightarrow \mathrm{C} \rightarrow ...$, whose members' decay constants are $\lambda_\mathrm{A}$, $\lambda_\mathrm{B}$, $\lambda_\mathrm{C}$, etc. Since the nuclide A is not replenished, the number of nuclei of type A decreases exponentially with time according to (4.1.3)

$$N_\mathrm{A}(t) = N_\mathrm{A}(0)\mathrm{e}^{-\lambda_\mathrm{A} t}. \tag{4.2.1}$$

Since nuclei of the type B do not only decay, but are also created (due to decay of the parent nuclide A), the differential equation describing the time variation of the number of nuclei of type B has an additional positive term, which reflects the decay of the nuclide A:

$$\frac{\mathrm{d}N_\mathrm{B}}{\mathrm{d}t} = -\lambda_\mathrm{B} N_\mathrm{B} + \lambda_\mathrm{A} N_\mathrm{A}. \tag{4.2.2}$$

The time function $N_\mathrm{B}(t)$ can be derived as follows. The first term on the right-hand side of Equation (4.2.2) is transferred to the left-hand side, and then both sides of the equation are multiplied by $\mathrm{e}^{\lambda_\mathrm{B} t}$. According to the rule of calculating the derivative of a product of two functions, the expression on the left-hand side of the resulting equation is the time derivative of $N_\mathrm{B}\mathrm{e}^{\lambda_\mathrm{B} t}$:

$$\frac{\mathrm{d}}{\mathrm{d}t}(N_\mathrm{B}\mathrm{e}^{\lambda_\mathrm{B} t}) = \lambda_\mathrm{A} N_\mathrm{A}\mathrm{e}^{\lambda_\mathrm{B} t}. \tag{4.2.3}$$

By substituting (4.2.1) for $N_\mathrm{A}(t)$, we obtain:

$$\frac{\mathrm{d}}{\mathrm{d}t}(N_\mathrm{B}\mathrm{e}^{\lambda_\mathrm{B} t}) = \lambda_\mathrm{A} N_\mathrm{A}(0)\mathrm{e}^{(\lambda_\mathrm{B}-\lambda_\mathrm{A})t}. \tag{4.2.4}$$

After integrating,

$$N_\mathrm{B}\mathrm{e}^{\lambda_\mathrm{B} t} = \lambda_\mathrm{A} N_\mathrm{A}(0)\int \mathrm{e}^{(\lambda_\mathrm{B}-\lambda_\mathrm{A})t}\mathrm{d}t = \frac{\lambda_\mathrm{A}}{\lambda_\mathrm{B}-\lambda_\mathrm{A}} N_\mathrm{A}(0)\mathrm{e}^{(\lambda_\mathrm{B}-\lambda_\mathrm{A})t} + K, \tag{4.2.5}$$

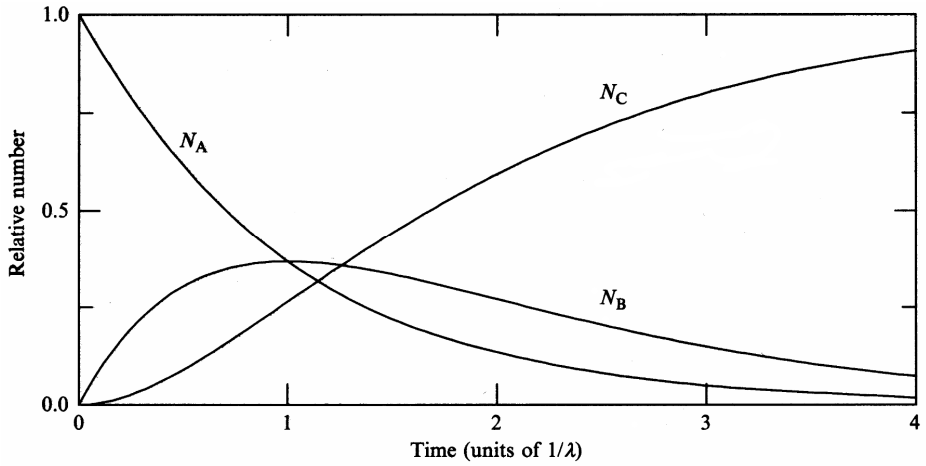


**Fig. 4.1.** Variation with time of the amount of nuclides A, B and C in a decay chain A → B → C, where $\lambda_A = \lambda_B = \lambda$ and C is stable. Note that $N_A + N_B + N_C = 1$ at any time.

where $K$ is the integration constant. It depends on initial conditions. If there were no nuclei of type B at the initial moment of time (i.e., $N_B(0) = 0$), then it follows from (4.2.5) that

$$K = -\frac{\lambda_A}{\lambda_B - \lambda_A} N_A(0) . \tag{4.2.6}$$

By substituting (4.2.6) for $K$ in (4.2.5), the final result is obtained:

$$N_B(t) = \frac{\lambda_A}{\lambda_B - \lambda_A} N_A(0)(e^{-\lambda_A t} - e^{-\lambda_B t}) . \tag{4.2.7}$$

Differential equations similar to Equation (4.2.3) describe the time dependences of all subsequent members of the decay chain, too. Fig. 4.1 shows time dependences of the numbers of nuclides of type A, B and C when $\lambda_A = \lambda_B = \lambda$, and C is a stable nuclide.

If the half-life of the daughter nuclide is much larger than the half-life of the parent nuclide (i.e., the decay constant is much less: $\lambda_B << \lambda_A$), then it may be assumed that the decay of the mixture of the two nuclides is a two-stage process. First, almost all nuclei of type A decay rapidly, transforming into nuclei of type B (A → B), and then nuclei of type B decay slowly (B → C). In this case, after a time that is much longer than $1 / \lambda_A$, it follows from Equation (4.2.7) that

$$N_B(t) \approx N_A(0) e^{-\lambda_B t} . \tag{4.2.8}$$

In another case, when the parent nuclide has a longer half-life than the daughter nuclide ($\lambda_A < \lambda_B$), the number $N_B$ at first increases, and finally (after a time that is long enough to ensure that $e^{-\lambda_A t} >> e^{-\lambda_B t}$), the following approximate equality becomes true:

$$N_B(t) \approx \frac{\lambda_A}{\lambda_B - \lambda_A} N_A(0) e^{-\lambda_A t} \equiv \frac{\lambda_A}{\lambda_B - \lambda_A} N_A(t) \tag{4.2.9}$$

(the larger the value of $t$, the more precise this approximate equality). Thus, if the parent nuclide is longer-lived than the daughter nuclide, the so-called ***radioactive equilibrium*** is eventually established: the *ratio* of quantities of both nuclides is constant and equal to

$$\frac{N_B}{N_A} = \frac{\lambda_A}{\lambda_B - \lambda_A} . \tag{4.2.10}$$

If $\lambda_A << \lambda_B$, then

$$\frac{N_B}{N_A} \approx \frac{\lambda_A}{\lambda_B} = \frac{T_B}{T_A} , \tag{4.2.11}$$

where $T_B$ and $T_A$ are half-lives of nuclides A and B. The latter equality can be rewritten as $\lambda_A N_A \approx \lambda_B N_B$. According to (4.1.4), the products $\lambda_A N_A$ and $\lambda_B N_B$ are activities of nuclides A and B, respectively. Thus, if the half-life of the parent nuclide is much longer than the half-lives of all radioactive daughter nuclides, than the condition of radioactive equilibrium can be formulated as follows: *at radioactive equilibrium, activities of all radioactive nuclides belonging to the same decay chain are equal***.**

If the half-life of the starting nuclide of a decay chain is much longer than half-lives of all daughter nuclides, then under conditions of radioactive equilibrium the equality (4.2.11) is true for *any* two nuclides of the same decay chain (with the condition that there is no "branching" of the decay chain,

i.e., there are no alternative decay channels, or the probability of one decay channel is much greater than probabilities of all other channels). This can be explained as follows. If nuclide B is in equilibrium with nuclide A, then, as it follows from Eq. (4.2.11), the rate of decay of B (i.e., $\lambda_B N_B$) is equal to the rate of its production (i.e., $\lambda_A N_A$). This means that $N_B$ decreases with the same decay constant (and half-life) as $N_A$. If the half-life of nuclide A is much longer than the duration of an experiment, then $N_A$ and $N_B$ (as well as activities $\lambda_A N_A$ and $\lambda_B N_B$) are practically constant during the experiment. If the rate of production of any radioactive nuclide is constant, then the rate of its decay increases, asymptotically approaching the rate of production (this can be proven mathematically by solving Eq. (4.2.2) with $\lambda_A N_A$ replaced by an arbitrary positive constant, which has the meaning of the production rate of nuclide B). This means that its quantity will eventually become practically constant, too, *regardless of its decay half-life*. Since the third member of the decay chain (nuclide C) is produced by decay of nuclide B, the rate of production of C is equal to the rate of decay of B, i.e., to $\lambda_B N_B$. Since the latter is practically constant, the rate of decay C (i.e., $\lambda_C N_C$) will also eventually become equal to $\lambda_B N_B$. Thus, the following equation is obtained:

$$\frac{N_C}{N_B} \approx \frac{\lambda_B}{\lambda_C} = \frac{T_C}{T_B}. \qquad (4.2.12)$$

The reasoning leading to this result is based only on the assumption that $T_A >> T_B$ and $T_A >> T_C$, but there is no restriction on the value of $T_B / T_C$ (for example, $T_B$ may be less than $T_C$). By applying the same reasoning to the further members of the decay chain, the relations similar to (4.2.12) are obtained for any other pair of nuclides (for example, C and D, D and E, etc.), including non-neighboring members of the decay chain (for example, B and D, A and C, A and D, etc.), as long half-lives of all daughter nuclides (B, C, D, etc.) are much less than $T_A$. The values of $T_B$, $T_C$, $T_D$, etc. determine only the time needed for a particular daughter nuclide (B, C, D, etc.) to attain radioactive equilibrium with nuclide A: this time can be approximately obtained by multiplying the maximum half-life of all daughter nuclides starting with nuclide B and ending with the current nuclide (B, C, D, etc.) by a factor of 4 or 5.

The most frequently encountered types of radioactive decay are alpha decay and beta decay. Among those types of radioactive decay, only the alpha decay causes a change of the mass of the nucleus (the mass number decreases by 4). Therefore, by expressing the mass numbers of nuclei as $A = 4n + k$, the term $k$ will be the same for all members of a given decay chain (the possible values of $k$ are 0, 1, 2 and 3). This means that there are four types of decay chains, each one corresponding to a particular value of $k$. Accordingly, all radioactive nuclides can be grouped into four categories, which are called ***radioactive families*** or ***decay families***. The starting isotope of each radioactive family is defined as the nuclide which has the longest half-live (although this nuclide itself may be a product of decay of other nuclides). Only three of the mentioned four decay families have been found in nature. The starting isotopes of those families have not completely decayed since formation of Earth. Those are the ***thorium series*** ($A = 4n$, starting isotope – the isotope of thorium $^{232}$Th), the ***uranium series*** ($A = 4n + 2$, starting isotope – the isotope of uranium $^{238}$U), and the ***actinium series*** ($A = 4n + 3$, starting isotope – the isotope of uranium $^{235}$U). The final nuclides of those three families are stables isotopes of lead ($^{208}$Pb, $^{206}$Pb and $^{207}$Pb, respectively). The fourth family – the ***neptunium series*** ($A = 4n + 1$, starting isotope – the isotope of neptunium $^{237}$Np) – does not naturally occur, because half-lives of all its members are much shorter than the age of Earth (e.g., half-life of $^{237}$Np is $2.14 \cdot 10^6$ years). The final nuclide of the neptunium series can be assumed to be the isotope of bismuth $^{209}$Bi, because its half-life is so long that it is practically stable (this half-life is $2 \cdot 10^{19}$ years). The main nuclides of each series are listed in Tables 4.1a–d.

Equations (4.2.11) and (4.2.12) can be applied to the decay chain starting with the isotope of radium $^{226}$Ra. Its half-live is 1622 years, whereas the half-live of the longest-lived daughter nuclide (isotope of lead $^{210}$Pb) is 22 years (see Table 4.1b). Consequently, if the time that passed since formation of the source material (containing $^{226}$Ra) is much longer than 22 years and if the source is hermetically sealed (so that radon $^{222}$Rn, which is an inert gas, does not escape to the environment), then all nuclides of this decay chain are at equilibrium and the quantity of each nuclide is directly proportional to its half-life, i.e., inversely proportional to its decay constant (according to (4.2.11) and (4.2.12)). If the age of the source material is not much longer than 22 years, then only the nuclides that are between $^{226}$Ra and $^{210}$Pb are at equilibrium (see Table 4.1b). Table 4.1e is a part of Table 4.1b containing only the main members of the $^{226}$Ra decay chain (this table omits nuclides $^{218}$At, $^{218}$Rn, $^{210}$Tl and $^{206}$Tl, which are formed by alternative decay channels, whose probability is very low).

**Table 4.1a**. Thorium series ($A = 4n$)

| Nuclide | Decay type | Half-life | Decay energy (MeV) | Daughter nuclide |
|---|---|---|---|---|
| $^{232}$Th | α | $1.405 \cdot 10^{10}$ y. | 4.081 | $^{228}$Ra |
| $^{228}$Ra | $\beta^-$ | 5.75 y. | 0.046 | $^{228}$Ac |
| $^{228}$Ac | $\beta^-$ | 6.25 h | 2.124 | $^{228}$Th |
| $^{228}$Th | α | 1.9116 y. | 5.520 | $^{224}$Ra |
| $^{224}$Ra | α | 3.6319 d. | 5.789 | $^{220}$Rn |
| $^{220}$Rn | α | 55.6 s | 6.404 | $^{216}$Po |
| $^{216}$Po | α | 0.145 s | 6.906 | $^{212}$Pb |
| $^{212}$Pb | $\beta^-$ | 10.64 h | 0.570 | $^{212}$Bi |
| $^{212}$Bi | $\beta^-$ (64.06 %)<br>α (35.94 %) | 60.55 min | 2.252<br>6.208 | $^{212}$Po<br>$^{208}$Tl |
| $^{212}$Po | α | 299 ns | 8.955 | $^{208}$Pb |
| $^{208}$Tl | $\beta^-$ | 3.053 min | 4.999 | $^{208}$Pb |
| $^{208}$Pb | – | stable | – | – |

**Table 4.1b**. Uranium series ($A = 4n + 2$)

| Nuclide | Decay type | Half-life | Decay energy (MeV) | Daughter nuclide |
|---|---|---|---|---|
| $^{238}$U | α | $4.468 \cdot 10^{9}$ y. | 4.270 | $^{234}$Th |
| $^{234}$Th | $\beta^-$ | 24.10 d. | 0.273 | $^{234}$Pa |
| $^{234}$Pa | $\beta^-$ | 6.70 h | 2.197 | $^{234}$U |
| $^{234}$U | α | 245500 y. | 4.859 | $^{230}$Th |
| $^{230}$Th | α | 75380 y. | 4.770 | $^{226}$Ra |
| $^{226}$Ra | α | 1602 y. | 4.871 | $^{222}$Rn |
| $^{222}$Rn | α | 3.8235 d. | 5.590 | $^{218}$Po |
| $^{218}$Po | α (99.98 %)<br>$\beta^-$ (0.02 %) | 3.10 min | 6.115<br>0.265 | $^{214}$Pb<br>$^{218}$At |
| $^{214}$Pb | $\beta^-$ | 26.8 min | 1.024 | $^{214}$Bi |
| $^{218}$At | α (99.90 %)<br>$\beta^-$ (0.10 %) | 1.5 s | 6.874<br>2.883 | $^{214}$Bi<br>$^{218}$Rn |
| $^{218}$Rn | α | 35 ms | 7.263 | $^{214}$Po |
| $^{214}$Bi | $\beta^-$ (99.98 %)<br>α (0.02 %) | 19.9 min | 3.272<br>5.617 | $^{214}$Po<br>$^{210}$Tl |
| $^{214}$Po | α | 0.1643 ms | 7.883 | $^{210}$Pb |
| $^{210}$Tl | $\beta^-$ | 1.30 min | 5.484 | $^{210}$Pb |
| $^{210}$Pb | $\beta^-$ | 22.3 y. | 0.064 | $^{210}$Bi |
| $^{210}$Bi | $\beta^-$ (99.99987 %)<br>α (0.00013 %) | 5.013 d. | 1.426<br>5.982 | $^{210}$Po<br>$^{206}$Tl |
| $^{210}$Po | α | 138.376 d. | 5.407 | $^{206}$Pb |
| $^{206}$Tl | $\beta^-$ | 4.199 min | 1.533 | $^{206}$Pb |
| $^{206}$Pb | – | stable | – | – |

**Table 4.1c**. Actinium series ($A = 4n + 3$)

| Nuclide | Decay type | Half-life | Decay energy (MeV) | Daughter nuclide |
|---|---|---|---|---|
| $^{235}$U | α | $7.04 \cdot 10^8$ y. | 4.678 | $^{231}$Th |
| $^{231}$Th | $\beta^-$ | 25.52 h | 0.391 | $^{231}$Pa |
| $^{231}$Pa | α | 32760 y. | 5.150 | $^{227}$Ac |
| $^{227}$Ac | $\beta^-$ (98.62 %)<br>α (1.38 %) | 21.772 y. | 0.045<br>5.042 | $^{227}$Th<br>$^{223}$Fr |
| $^{227}$Th | α | 18.68 d. | 6.147 | $^{223}$Ra |
| $^{223}$Fr | $\beta^-$ | 22.00 min | 1.149 | $^{223}$Ra |
| $^{223}$Ra | α | 11.43 d. | 5.979 | $^{219}$Rn |
| $^{219}$Rn | α | 3.96 s | 6.946 | $^{215}$Po |
| $^{215}$Po | α (99.99977 %)<br>$\beta^-$ (0.00023 %) | 1.781 ms | 7.527<br>0.715 | $^{211}$Pb<br>$^{215}$At |
| $^{215}$At | α | 0.1 ms | 8.178 | $^{211}$Bi |
| $^{211}$Pb | $\beta^-$ | 36.1 min | 1.367 | $^{211}$Bi |
| $^{211}$Bi | α (99.724 %)<br>$\beta^-$ (0.276 %) | 2.14 min | 6.751<br>0.575 | $^{207}$Tl<br>$^{211}$Po |
| $^{211}$Po | α | 516 ms | 7.595 | $^{207}$Pb |
| $^{207}$Tl | $\beta^-$ | 4.77 min | 1.418 | $^{207}$Pb |
| $^{207}$Pb | – | stable | – | – |

**Table 4.1d**. Neptunium series ($A = 4n + 1$)

| Nuclide | Decay type | Half-life | Decay energy (MeV) | Daughter nuclide |
|---|---|---|---|---|
| $^{237}$Np | α | $2.14 \cdot 10^6$ y. | 4.959 | $^{233}$Pa |
| $^{233}$Pa | $\beta^-$ | 27.0 d. | 0.571 | $^{233}$U |
| $^{233}$U | α | $1.592 \cdot 10^5$ y. | 4.909 | $^{229}$Th |
| $^{229}$Th | α | $7.54 \cdot 10^4$ y. | 5.168 | $^{225}$Ra |
| $^{225}$Ra | $\beta^-$ | 14.9 d. | 0.36 | $^{225}$Ac |
| $^{225}$Ac | α | 10.0 d. | 5.935 | $^{221}$Fr |
| $^{221}$Fr | α | 4.8 min | 6.3 | $^{217}$At |
| $^{217}$At | α | 32 ms | 7.0 | $^{213}$Bi |
| $^{213}$Bi | α | 45.6 min | 5.87 | $^{209}$Tl |
| $^{209}$Tl | $\beta^-$ | 2.2 min | 3.99 | $^{209}$Pb |
| $^{209}$Pb | $\beta^-$ | 3.25 h | 0.644 | $^{209}$Bi |
| $^{209}$Bi | α | $1.9 \cdot 10^{19}$ y. | 3.14 | $^{205}$Tl |
| $^{205}$Tl | – | stable | – | – |

**Table 4.1e**. The main nuclides of the $^{226}$Ra decay chain

| Nuclide | Decay type | Half-life | Energy of α particles (MeV) |
|---|---|---|---|
| $^{226}$Ra | α | 1602 y. | 4.78 |
| $^{222}$Rn | α | 3.825 d. | 5.49 |
| $^{218}$Po | α | 3.05 min | 6.00 |
| $^{214}$Pb | $\beta^-$ | 26.8 min | – |
| $^{214}$Bi | $\beta^-$ | 19.7 min | – |
| $^{214}$Po | α | $1.6 \cdot 10^{-4}$ s | 7.68 |
| $^{210}$Pb | $\beta^-$ | 22 y. | – |
| $^{210}$Bi | $\beta^-$ | 5.01 d. | – |
| $^{210}$Po | α | 138.4 d. | 5.30 |
| $^{206}$Pb | stable | | |

# 5. Alpha decay

## 5.1. Main properties of alpha decay

During α emission, the parent nucleus loses both mass and charge:

$$(A, Z) \rightarrow (A - 4, Z - 2).$$

A generalized equation of α decay:

$$^{A}_{Z}\mathrm{X} \rightarrow {}^{A-4}_{Z-2}\mathrm{Y} + {}^{4}_{2}\mathrm{He}$$

An example:

$$^{226}_{88}\mathrm{Ra} \rightarrow {}^{222}_{86}\mathrm{Rn} + {}^{4}_{2}\mathrm{He}$$

Main properties of α decay:

1. $Z > 82$.
2. Discrete energies of α particles emitted by a particular nuclide.
3. Narrow energy range of emitted α particles: $E = (4 - 8{,}7)$ MeV.
4. Very strong dependence of the decay half-life on the particle energy $E$. It is given by the ***Geiger and Nuttall law*** of alpha decay:

$$\lg t_{1/2} = C + \frac{D}{\sqrt{E}}$$

Property No. 1 is related to the fact that α decay is caused by Coulomb repulsion of protons.

The emitted particle is an α particle (and not, e.g., a proton), because, when an α particle is emitted from a nucleus, the total rest mass of the system decreases. The decay energy ($Q_\alpha$) is released in the form of kinetic energies of the daughter nucleus and the α particle:

$$Q_\alpha = (m_\mathrm{P} - m_\mathrm{D} - m_\alpha)c^2 = E_\mathrm{D} + E_\alpha$$

As evident from the table below, the decay energy is only positive for the case when the emitted particle is an α particle, hence this is the only possible type of spontaneous decay.

**Table 5.1** Decay energy for various types of decay of the $^{232}$U nucleus

| Emitted particle | Decay energy (MeV) | Emitted particle | Decay energy (MeV) |
|---|---|---|---|
| n | –7.26 | $^{4}$He | +5.41 |
| $^{1}$H | –6.12 | $^{5}$He | –2.59 |
| $^{2}$H | –10.70 | $^{6}$He | –6.19 |
| $^{3}$H | –10.24 | $^{6}$Li | –3.79 |
| $^{3}$He | –9,92 | $^{7}$Li | –1,94 |

Property No. 2 is caused by discrete energy levels of the daughter nucleus (see Fig. 5.1).

Properties No. 3 and 4 are explained by the semi-classical theory of α decay by G. Gamow (1928).

Potential energy of the alpha particle (see Fig. 5.2):

$$U(x) \approx \begin{cases} Ze^2/(2\pi\varepsilon_0 x), & \text{kai } x > d, \\ U_0 < 0, & \text{kai } x \le d. \end{cases}$$

Height of the Coulomb potential barrier:

$$U_{\max} \approx U(d) = \frac{Ze^2}{2\pi\varepsilon_0 d}$$

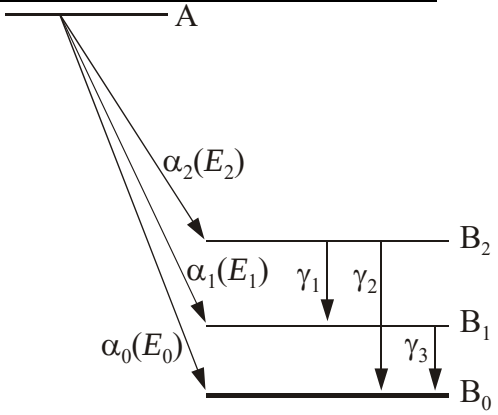


**Fig. 5.1.** Explanation of the discrete character of α particle velocity distribution

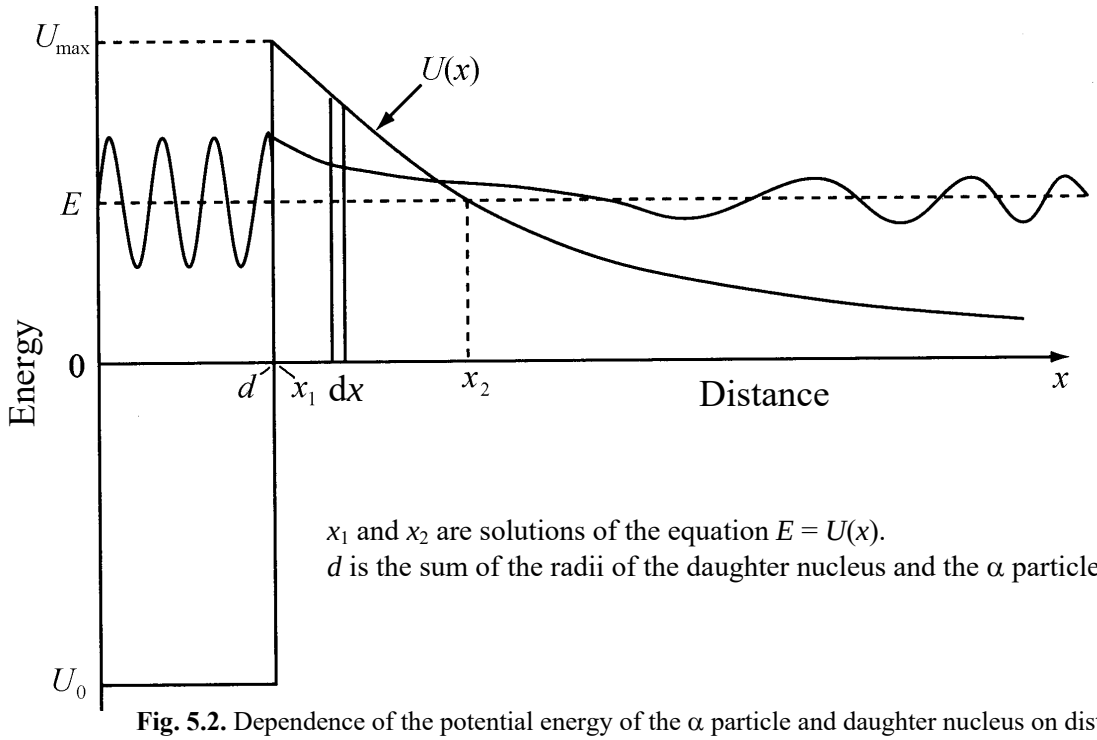


$x_1$ and $x_2$ are solutions of the equation $E = U(x)$.
$d$ is the sum of the radii of the daughter nucleus and the α particle. $x_1 \approx d$

**Fig. 5.2.** Dependence of the potential energy of the α particle and daughter nucleus on distance

## 5.2. Wave function of a free particle and quantum tunneling

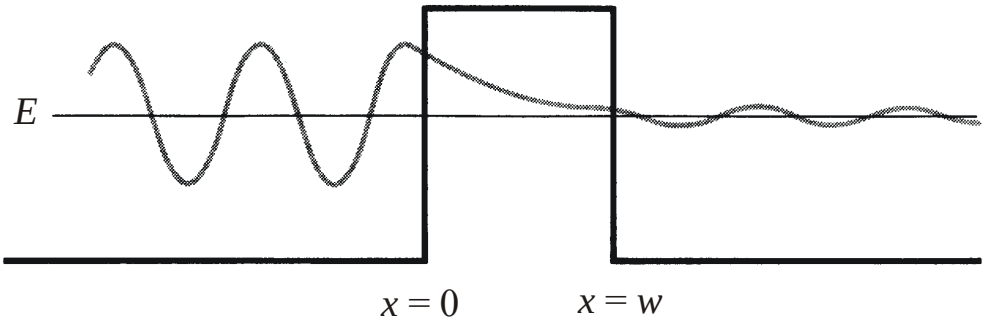


**Fig. 5.3.** Wave function of a particle when there is a potential barrier, whose height exceeds the particle energy $E$

One-dimensional Schrödinger equation:

$$\frac{\mathrm{d}^2\psi}{\mathrm{d}x^2} = \frac{2m}{\hbar^2}(U(x) - E)\psi$$

In the case of a rectangular potential barrier (see Fig. 5.3), the Schrödinger equation is:

$$\frac{\mathrm{d}^2\psi_1}{\mathrm{d}x^2} + k_1^2\psi_1 = 0 \quad \text{(I region)},$$

$$\frac{\mathrm{d}^2\psi_2}{\mathrm{d}x^2} - k_2^2\psi_2 = 0 \quad \text{(II region)},$$

$$\frac{\mathrm{d}^2\psi_3}{\mathrm{d}x^2} + k_1^2\psi_3 = 0 \quad \text{(III region)}.$$

$$k_1 = \frac{\sqrt{2mE}}{\hbar}, \quad k_2 = \frac{\sqrt{2m(U_0 - E)}}{\hbar}$$

The general solution:

$$\psi_1 = A\exp(\mathrm{i}k_1x) + B\exp(-\mathrm{i}k_1x) \quad \text{(I region)},$$

$$\psi_2 = C\exp(k_2x) + D\exp(-k_2x) \quad \text{(II region)},$$

$$\psi_3 = F\exp(\mathrm{i}k_1x) + G\exp(-\mathrm{i}k_1x) \quad \text{(III region)}.$$

If the particle source is at $x = -\infty$, then

$$G = 0$$

$A$ is the amplitude of the *incident* wave, $B$ is the amplitude of the *reflected* wave, and $F$ is the amplitude of the *transmitted* wave.

The amplitude ($A$, $B$, or $F$) defines the particle ***flux density***. E.g., if a particle is incident on the potential barrier, then its flux density is

$$i = N\frac{\hbar k}{m}|A|^2 .$$

The transmission probability is defined as the ratio of transmitted and incident flux densities:

$$S \equiv \frac{|F|^2}{|A|^2}.$$

By applying the continuity conditions to the functions $\psi_1$, $\psi_2$ and $\psi_3$ and assuming that

$$k_2 w >> 1,$$

(i.e., a high and wide potential barrier), the following expression of $S$ is obtained:

$$S \approx \exp\left[-\frac{2}{\hbar}\sqrt{2m(U_0 - E)}\cdot w\right] << 1$$

Such effect when a particle "tunnels" through a potential barrier that it classically can not surmount is called ***quantum tunneling***.

A wide potential barrier of any shape can be constructed as a sequence of a large number $N$ of thin potential rectangular barriers. Hence, the transmission probability of such a barrier is

$$S \approx \lim_{N\to\infty}\prod_{n=1}^{N} S_n \approx \exp\left[-\frac{2}{\hbar}\int_{x_1}^{x_2}\sqrt{2m(U(x)-E)}\,\mathrm{d}x\right]$$

## 5.3. Derivation of the Geiger-Nuttall law from the expression for transmission probability

Solutions of equation $U(x) = E$:

$$x_1 \approx d \approx 10^{-14}\ \mathrm{m}$$

$$x_2 = \frac{Ze^2}{2\pi\varepsilon_0 E}$$

We can imagine the α particle moving back and forth inside the nucleus with a speed $\upsilon$ and presenting itself at the barrier with a frequency ($\upsilon / d$). Then the decay constant $\lambda$ can be obtained by multiplying this frequency and the transmission probability $S$:

$$\lambda \approx \frac{\upsilon}{d}S$$

$E = M\upsilon^2/2$. When $E = 10$ MeV, $\upsilon \approx 2\cdot 10^7$ m/s. Therefore,

$$\lambda \approx 10^{21}\cdot S \quad [\mathrm{s}^{-1}]$$

Since

$$t_{1/2} = \frac{\ln 2}{\lambda},$$

we obtain

$$\lg t_{1/2} \approx B - 0.434\ln S,$$

where $t_{1/2}$ is expressed in seconds, and $B \approx -21$. Dependence of $\ln S$ on $E$ is obtained on the basis of the simplifying assumption that $E << U$ inside the barrier:

$$-\int_{x_1}^{x_2}\sqrt{2m(U(x)-E)}\,\mathrm{d}x \approx -\int_{x_1}^{x_2}\sqrt{2mU(x)}\,\mathrm{d}x = -\int_{x_1}^{x_2}\sqrt{2m\frac{Ze^2}{2\pi\varepsilon_0 x}}\,\mathrm{d}x = const(\sqrt{x_1} - \sqrt{x_2}) \sim -\frac{1}{\sqrt{E}}$$

(because $x_2 \sim 1/E$, and $x_1$ is approximately constant). Hence,

$$\lg t_{1/2} = C + \frac{D}{\sqrt{E}}\,.$$

# 6. Detecting heavy charged particles

6.1. *Interaction of heavy charged particles with matter*

In nuclear physics, the term "heavy particles" is applied to particles with mass that is much larger than electron mass ($m_e = 9{,}1 \cdot 10^{-31}$ kg). Examples of heavy particles are the proton (charge $+e$, mass $m_p = 1{,}67 \cdot 10^{-27}$ kg) and various nuclei (for example, $^4$He nucleus, which is composed of two protons and two neutrons).

When radiation is composed of charged particles, the main quantity characterizing interaction of radiation with matter is the average decrease of particle kinetic energy per unit path length. This quantity is called the ***stopping power*** of the medium and is denoted $S$. An alternative notation is $-\mathrm{d}E/\mathrm{d}x$ or $|\mathrm{d}E/\mathrm{d}x|$ (such notation reflects the mathematical meaning of the stopping power: it is opposite to the derivative of particle energy $E$ relative to the traveled path $x$).

The main mechanism of the energy loss of heavy charged particles (and electrons with energies of the order of a few MeV or less) is ionization or excitation of the atoms of matter (*excitation* is the process when internal energy of the atom increases, but it does not lose any electrons). All such energy losses are collectively called ***ionization energy losses*** (this term is applied to energy losses due to excitation, too). Atoms that are excited or ionized due to interaction with a fast charged particle lie close to the trajectory of the incident particle (at a distance of a few nanometers from it). The nature of the interaction that causes ionization or excitation of atoms is the so-called Coulomb force which acts between the incident particles and electrons of the matter. When an incident charged particle passes by an atom, it continuously interacts with the electrons of the atom. For example, if the incident particle has a positive electric charge, it continuously "pulls" the electrons (whose charge is negative) toward itself (see Fig. 6.1). If the pulling force is sufficiently strong and if its time variation is sufficiently fast (i. e. if the incident particle's velocity is sufficiently large), then some of the electrons may by liberated from the atom (i. e., the atom may be ionized). Alternatively, the atom may be excited to higher energy levels without ionization.

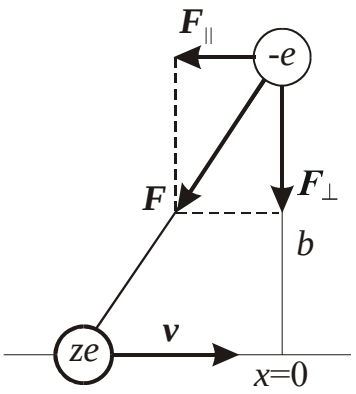


**Fig. 6.1.** The classical model of ionization of an atom due to Coulomb interaction of its electrons with an incident heavy charged particle. $ze$ is the electric charge of the incident particle, $-e$ is the electron charge

Coulomb interaction of the incident particles with atomic nuclei is also possible, but it has a much smaller effect on the motion of the incident charged particles, because the nuclei of the material occupy only about $10^{-15}$ of the volume of their atoms.

Using the laws of conservation of energy and momentum, it can be proved that the largest energy that a non-relativistic particle with mass $M$ can transfer to an electron with mass $m_e$ is equal to $4m_eE/M$, where $E$ is kinetic energy of the particle. Using the same laws, it can be shown that the largest possible angle between the direction of particle motion after the interaction and its direction prior to the interaction is equal to $m_e / M$. Since $M$ exceeds $m_e$ by three orders of magnitude (see above), we can conclude that the decrease of energy of a heavy charged particle due to a single excitation or ionization event is much smaller than the total kinetic energy of the particle and the incident particle practically does not change its direction of motion when it interacts with an atom (i. e., the trajectories of heavy charged particles in matter are almost straight). *Note*: The change of the direction of particle motion is called ***scattering***.

The quantum mechanical calculation of the mentioned interaction gives the following expression of the stopping power due to ionization energy losses:

$$S = \frac{1}{4\pi\varepsilon_0^2}\frac{z^2e^4n}{m_e\upsilon^2}\left\{\ln\frac{2m_e\upsilon^2}{\bar{I}(1-\beta^2)} - \beta^2\right\}, \qquad (6.1.1)$$

where $\upsilon$ is the particle velocity, $z$ is its charge in terms of elementary charge $e$ ("elementary charge" $e$ is the absolute value of electron charge), $n$ is the electron concentration in the material, $m_e$ is electron mass, $\varepsilon_0$ is the electric constant ($\varepsilon_0 = 8{,}854 \cdot 10^{-12}$ F/m), $\beta$ is the ratio of particle velocity and velocity of light $c$ (i. e. $\beta \equiv \upsilon / c$), and the parameter $\bar{I}$ is the mean excitation energy of the atomic electrons (i. e., the mean

value of energies needed to cause all possible types of excitation and ionization of the atom). This formula is applicable when $v$ exceeds $10^7$ m/s (this corresponds to alpha particle energy of 2 MeV).

The strong dependence of the stopping power (6.1.1) on particle velocity $v$, its charge $z$ and electron concentration $n$ can be explained as follows. The decrease of particle energy during one interaction is directly proportional to the square of the momentum transferred to the atomic electron (this follows from the general expression of kinetic energy via the momentum). This momentum is proportional to duration of the interaction (this follows from the second Newton's law), and the latter duration is inversely proportional to $v$. Therefore the mean decrease of particle energy in one interaction, (and the stopping power) is inversely proportional to $v^2$. The proportionality of the stopping power to $z^2$ follows from the fact that the mentioned momentum transfer is directly proportional to Coulomb force, which is proportional to $z$ according to the Coulomb's law. The proportionality of the stopping power to $n$ follows from the fact that the mean number of collisions per unit path is proportional to $n$.

The expressions of stopping power (6.1.1) does not include the mass of the incident particle. This means that ionization stopping powers of different particles with equal velocity and equal absolute values of electric charge $z$ (for example, electron and proton) are equal. However, stopping powers of electrons and protons with equal *energies* are very different. This is because velocity of a particle with a given energy is strongly dependent on the particle mass. For example, velocity $v$ and kinetic energy $E$ of a non-relativistic particle are related as follows:

$$v^2 = \frac{2E}{M}, \tag{6.1.2}$$

where $M$ is the particle mass. After replacing $v^2$ in Eq. (6.1.1) with the expression (6.1.2) and taking into account that for non-relativistic particles $\beta << 1$, we obtain:

$$S = \frac{1}{8\pi\varepsilon_0^2}\frac{z^2 e^4 nM}{m_e E}\ln\frac{4m_e E}{\bar{I}M}. \tag{6.1.3}$$

We see that ionization energy losses of non-relativistic particles are directly proportional to the mass of the particle. Therefore, ionization stopping power of heavy charged particles (e. g. protons) is much larger than ionization stopping power of electrons with the same energy. For example, the stopping power for 0,5 MeV protons is about 2000 times larger than the stopping power for 0,5 MeV electrons. Hence, a heavy charged particle is able to travel a much smaller distance in a material than an electron with the same energy.

## 6.2. *Detector pulse height spectrum*

The most common method of measuring particle kinetic energy is based on the fact that the number of free charge carriers created due to absorption of particle's energy in a material is directly proportional to the absorbed energy. The mentioned number of carriers can be easily measured by applying a strong enough electric field which separates the opposite charge carriers (such as electrons and holes in a semiconductor or electrons and positive ions in a gas chamber) and collects them on the electrodes of a capacitor. This results in a voltage pulse whose height ($H$) is proportional to the collected charge and to the absorbed energy.

By measuring the heights of a large number of voltage pulses, we would notice that those heights are not equal to each other. In other words, those heights are statistically distributed. This distribution may be caused by imperfection of the detector (i. e., the pulse heights may have a random component even when the absorbed energy is exactly the

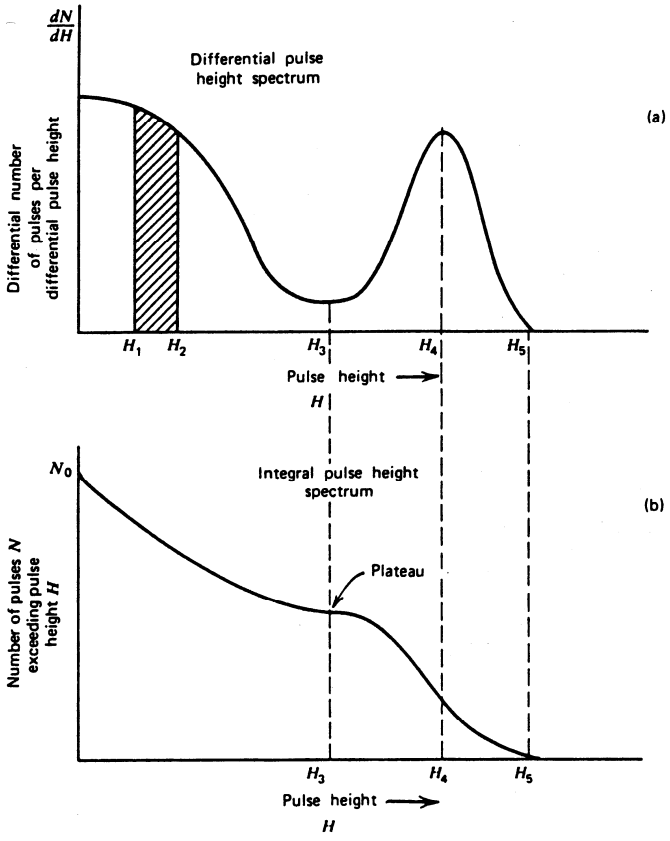


**Fig. 6.2.** Examples of differential and integral pulse height spectra

same), or it may reflect the distribution of the absorbed energy. Therefore, the pulse height distribution is frequently used when investigating the energies of incident particles or when evaluating quality of the detector.

The statistical distribution of pulse heights is usually represented in the form of a differential pulse height spectrum. An example of such a spectrum is shown in Fig. 6.2a. The horizontal axis corresponds to pulse height. The vertical axis corresponds to the number of pulses with a particular height. Let us denote this number as $\Delta n$. In order to define this number, it is necessary to define a particular interval of pulse heights. Let us denote the width of this interval as $\Delta H$. Thus, $\Delta n$ is the number of pulses with heights between $H$ and $H + \Delta H$. Now, let us take the ratio $\Delta n / \Delta H$. If the interval width $\Delta H$ is small enough, then the ratio $\Delta n / \Delta H$ would be the same as the ratio of infinitesimal differences (differentials) $\mathrm{d}n/\mathrm{d}H$. The latter ratio is plotted in Fig. 6.2a. The number of pulses with heights between $H_1$ and $H_2$ can be determined by integrating the differential pulse height spectrum from $H_1$ to $H_2$:

$$n(H_1 < H < H_2) = \int_{H_1}^{H_2} \frac{\mathrm{d}n}{\mathrm{d}H}\mathrm{d}H \ . \tag{6.2.1}$$

This integral is shown as a hatched area in Fig. 6.2a. The total number of pulses is equal to the integral of the entire differential pulse height spectrum:

$$n_0 = \int_0^{\infty} \frac{\mathrm{d}n}{\mathrm{d}H}\mathrm{d}H \ . \tag{6.2.2}$$

The largest pulse height is given by the abscissa ($x$-coordinate) of the right edge of the spectrum (for example, in the case of Fig. 6.2a the largest pulse height is $H_5$). The abscissas of the maxima (peaks) of the spectrum (e. g., $H_4$ in Fig. 6.2a) correspond to the most probable pulse heights, i. e. such pulse heights that are observed most frequently. The abscissas of the minima of the spectrum (e. g., $H_3$ in Fig. 6.2a) correspond to least probable pulse heights, i. e., pulse heights that are least likely to be observed.

The same information that is contained in a differential pulse height spectrum can be presented in the form of an *integral* pulse height spectrum. The integral pulse height spectrum gives the total number of pulses with heights greater than a specified value $H$. In other words, the integral pulse height spectrum is the integral of the differential pulse height spectrum from $H$ to $\infty$:

$$n(H) = \int_H^{\infty} \frac{\mathrm{d}n}{\mathrm{d}H}\mathrm{d}H \ . \tag{6.2.3}$$

$n(H)$ is always a decreasing function. The value of the integral pulse height spectrum at $H = 0$ is equal to the total number of pulses $n_0$. As in the case of the differential pulse height spectrum, the abscissa of the rightmost point of the integral pulse height spectrum is equal to the maximum pulse height (e. g., $H_5$ in Fig. 6.2b).

The differential and integral pulse height spectra are equivalent to each other in terms of the information that they provide. The value of the differential pulse height spectrum corresponding to any value of pulse height $H$ is equal to the absolute value of the slope (i. e. rate of decrease) of the integral spectrum corresponding to the same pulse height. The maxima of the differential spectrum correspond to the largest slope of the integral spectrum (e. g., point $H_4$ in Fig. 6.2). The minima of the differential spectrum correspond to the smallest slope of the integral spectrum (e. g., point $H_3$ in Fig. 6.2). In practice, the differential pulse height spectrum is used more frequently than the integral pulse height spectrum, because small changes of the spectrum can be more easily noticed in the differential spectrum than in the integral spectrum.

## 6.3. *Detector energy resolution*

Radiation detectors are frequently used for measurements of radiation energy spectrum. Such measurements comprise the field of ***radiation spectroscopy***. In this section, we will discuss two related concepts that are important in radiation spectroscopy – energy response function and energy resolution of a detector.

Let us assume that energy of all particles that enter the detector is equal to $E_0$. In the ideal case, the heights of all pulses caused by those particles should be also equal to each other and proportional to $E_0$:

$$H_0 = const \cdot E_0 \, . \tag{6.3.1}$$

However, as mentioned in Section 6.2, detector pulse heights are not equal to each other even when the incident particles have equal energies. As a result, the relation (6.3.1) only applies to the *average* pulse height. I. e., the average pulse height of a real detector is proportional to particle energy. The heights of individual pulses are randomly distributed about the average height. As mentioned, this distribution is usually presented in the form of a differential pulse height spectrum. The differential pulse height spectrum corresponding to a particular energy $E_0$ of incident particles is called the ***response function*** of the detector corresponding to particle energy $E_0$. We will denote this function $G(H; E_0)$. The pulse height $H$ is the argument of the response function, while the particle energy $E_0$ is its parameter. The shape of the response function is Gaussian:

$$G(H;E_0)=\frac{n_0}{\sigma\sqrt{2\pi}}\exp\left(-\frac{(H-H_0(E_0))^2}{2\sigma^2}\right), \qquad (6.3.2)$$

where $H_0$ is the average pulse height (given by (6.3.1)), $\sigma$ is the standard deviation of pulse height, and $n_0$ is the total number o pulses (i. e. the integral of the response function from $-\infty$ to $+\infty$). An example of a detector response function is shown in Fig. 6.3. The statistical uncertainty of pulse height is reflected by the width of the response function. This width ($\Delta H$) is usually measured at half-height of the peak (that is why it is abbreviated FWHM: "full width at half maximum"). If the peak is Gaussian in shape, then FWHM is related to the standard deviation of pulse height as follows:

$$\Delta H = 2{,}35\sigma .$$

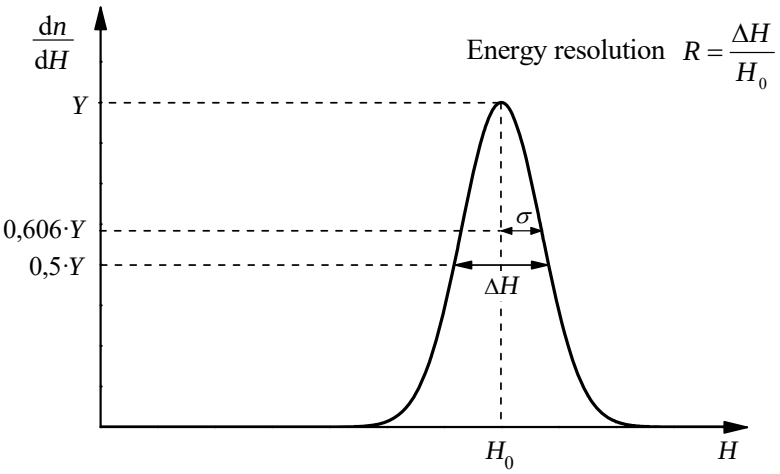


**Fig. 6.3.** Detector response function and definition of energy resolution

Fig. 6.4 shows an example of two response functions corresponding to the same particle energy $E_0$. Since the particle energy is the same in both cases, the position of the maximum ($H_0$) is the same, too ($H_0$ is the average pulse height). If the total number of pulses ($n_0$) is the same, too, then the *areas* (integrals) of both peaks are also equal to each other. However, it is obvious that the *widths* of those peaks are different. The larger width corresponds to worse *energy resolution*. A large width of a maximum means that the spread (uncertainty) of pulse heights was large, even though each interaction of a particle with the detector caused the same amount of energy to be transferred to the detector material. The energy resolution is defined as the ratio of the width at half-maximum to the average pulse height:

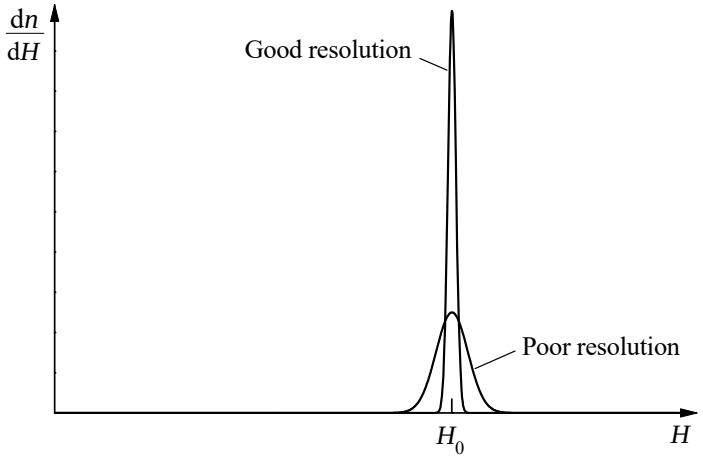


**Fig. 6.4.** Examples of response functions for detectors with relatively good resolution and relatively poor resolution

$$R=\frac{\Delta H}{H_0}. \qquad (6.3.3)$$

Energy resolution of semiconductor detectors that are used in alpha particle spectroscopy is less than 1 %. Energy resolution of scintillation detectors that are used in gamma ray spectroscopy is significantly worse: 5 % to 10 %. A smaller (better) energy resolution means that the detector can resolve two close peaks of the spectrum more easily. If the radiation is composed of particles with two values of energy, then the smallest difference of those two energies that can be resolved by a detector is approximately equal to $RE_0$, where $E_0$ is the arithmetic average of those two energies.

6.4. *Energy straggling of heavy charged particles*

As particles pass through matter, their energy distribution becomes wider. Therefore, the distribution of pulse heights caused by interaction of those particles with a detector material becomes wider, too. However, this does not imply that detector energy resolution deteriorates: energy resolution defines detector's response to particles *with a precisely defined energy*, and it characterizes the detector, not the incident radiation. As mentioned above, detector's energy resolution is important in situations when it is necessary to resolve two close peaks of the particles' energy spectrum. In this experiment, the analyzed energy spectrum has a roughly Gaussian shape (as in Fig. 6.3), and its width is much larger than the width of the detector response function. Under those conditions, the detector's energy resolution has practically no effect on the shape of the pulse height spectrum. I. e., it may be assumed that the width of the detector's response function approaches zero (this corresponds to the ideal detector). Then the detector pulse height distribution is determined only by distribution of particle energies. Thus, in this case the width of pulse height distribution can not be used to define energy resolution as in Fig. 6.3; instead, it defines the fluctuations of particle energies.

The widening of particles' energy distribution as they pass through matter is called ***energy straggling***. The reason of energy straggling is the random nature of a particle's interaction with an atom of the medium. This randomness means that the amount of energy that the particle loses due to its interaction with an atom of the material is random. This is evident from the model of the interaction described in Section 6.1: the energy transferred to an electron of the atom depends on distance $b$ between the electron and the particle (see Fig. 6.1), and this distance is a random quantity. The stopping power $S$ (also defined in Section 6.1) defines the rate of decrease of *average* energy (corresponding to the average pulse height, which is denoted $H_0$ in Fig. 6.3), but does not provide any information about the change of the width of the energy distribution. In earlier sections, the average energy was denoted $E$. Now, we will use this notation to denote the exact energy of a particle, whereas the statistical average of the energy will be denoted $\langle E \rangle$. The average energy $\langle E \rangle$ depends on distance $x$ that the particles have passed through the medium. If the initial energy of all particles was $E_0$, then their average energy after traveling the distance $x$ in a given material is equal to

$$\langle E(x) \rangle = E_0 - \int_0^x S(\langle E(x) \rangle) \mathrm{d}x \,, \tag{6.4.1}$$

where $S(\langle E \rangle)$ is the stopping power (it depends on the average energy). The particles with smaller energy have traveled a larger distance $x$, therefore they have experienced a larger number of collisions with atoms of the material, therefore their energy has a larger random component. It has been proven theoretically [4] that in the case of relatively large energy decrease (when the decrease $E_0 - \langle E \rangle$ is not much less than the initial energy $E_0$) the energy spectrum of heavy non-relativistic charged particles is roughly Gaussian in shape:

$$f(E;x) = \frac{n_0}{\sigma_E(x)\sqrt{2\pi}} \exp\left[ -\frac{(E - \langle E(x) \rangle)^2}{2\sigma_E^2(x)} \right]. \tag{6.4.2}$$

Interpretation of the energy spectrum $f(E; x)$ is similar to interpretation of the pulse height spectrum defined in Section 6.2. The main difference is that the argument of the energy spectrum is the particle energy $E$. The distance $x$ is the parameter of the function (6.4.2), i. e., the quantity that determines the position and width of the Gaussian peak. The area (integral) of the energy spectrum is equal to the total number of particles. The width of the peak at half-maximum is equal to

$$\Delta E(x) = 2.35 \sigma_E(x) \,,$$

where $\sigma_E(x)$ is the standard deviation of particles' energy after traveling distance $x$ in the material. It has been shown [4] that when both the initial energy $E_0$ and the average energy $\langle E(x) \rangle$ of alpha particles are between 1 MeV and 4 MeV, in the case of sufficiently large energy decrease (so that the Gaussian approximation (6.4.2) is valid) the following approximate expression of the squared standard deviation (variance) of the alpha particle energy can be used:

$$\sigma_E^2(x) \approx E_0^2 \frac{2m_\mathrm{e}}{3M} \left[ \ln\left( \frac{4m_\mathrm{e}E_0}{M\bar{I}} \right) \right]^{-1} \left[ \frac{E_0}{\langle E(x) \rangle} \right]^{1.33} \left\{ 1 - \left[ \frac{\langle E(x) \rangle}{E_0} \right]^3 \right\}. \tag{6.4.3}$$

# 7. Experimental setup and procedure

## 7.1. Introduction to the investigation technique

In this experiment, the energy spectrum of alpha particles is measured. The detector used for those measurements is a semiconductor detector (a silicon surface barrier detector), which generates a voltage pulse each time when an alpha particle strikes its front surface. The energy resolution of this detector is good enough, and the pulse height is proportional to particle energy (see Equation (6.3.1)), so that it can be assumed that the shape of the detector pulse height spectrum (discussed in Sections 6.2 and 6.3) accurately reflects the shape of the alpha particle energy spectrum (discussed in Section 6.4). The pulse height spectrum is measured using a device called a ***multichannel analyzer*** (MCA). It can be described as a number of counters with a common input, with each counter counting only the pulses whose heights belong to a specific narrow interval. This narrow interval of pulse heights is called a ***channel***. Channels are of equal width, they do not overlap and there are no gaps between them. Therefore, if a voltage pulse is applied to the input of the analyzer and if the height of this pulse is between the smallest and largest values that can be measured, then this pulse is counted by one (and *only* one) of the mentioned counters. Thus, the MCA sorts the pulses by their height. After measuring a large enough number of pulses, the pulse height spectrum is obtained. More precisely, the result of measurements is a set of numbers, one number per channel. Each number is the number of pulses whose height belongs to that channel. Let us denote this number $\delta n$. Bearing in mind the definition of the pulse height spectrum given in Section 6.2 (as the ratio $dn/dH$), it may seem that this set of numbers is not exactly the spectrum. However, it may be easily written in the conventional form: $\delta n = \delta n / \delta H$, where $\delta H = 1$. In other words, the channel width $\delta H$ should be chosen as the unit of pulse height.

In order to determine the particle energy spectrum from the pulse height spectrum, the detector has to be calibrated. The aim of calibration is determining the proportionality constant in the relation between particle energy and pulse height (6.3.1). In order to determine this constant, one has to measure the average pulse height when the detector is exposed to alpha particles of known energy $E_{\text{cal}}$. Then the energy $E$ of alpha particles that cause pulses of height $H$ can be calculated as follows:

$$E = \frac{E_{\text{cal}}}{H_{\text{cal}}} \cdot H \,. \tag{7.1}$$

In this experiment, an unsealed $^{241}$Am source is used for calibration. Here, the term “unsealed source” means that the emitted alpha particles do not lose energy in the source cover, hence the energy of alpha particles that reach the detector is equal to the energy of particles emitted from the $^{241}$Am nuclei (this energy is equal to 5.486 MeV). However, the $^{226}$Ra source is covered by a 2 μm-thick foil of gold and palladium alloy, where the alpha particles lose a part of their energy before entering the medium that surrounds the source. This is one of the reasons why the measured energies of alpha particles are significantly smaller than the true energies of particles emitted by $^{226}$Ra and its daughter nuclides (see Table 4.1e) the width of their spectrum is relatively large. Another factor that contributes to decrease of the average energy of alpha particles and to widening of their energy spectrum is the alpha particle energy loss in the gas that separates the source and the detector.

In addition to voltage pulses caused by alpha particles, the detector generates a large number of small pulses, which may be caused by external illumination and by thermal noise in the detector electronics. Besides, $^{241}$Am and some of the nuclides in the $^{226}$Ra decay chain emit gamma photons, which may also cause small pulses. In the measured pulse height spectra, those small pulses show up as a high peak in the region of small channel numbers (near the left edge of the spectrum). This peak has to be eliminated. This can be achieved by increasing the so-called ***discrimination level*** $H_{\text{d}}$ – the smallest pulse height that can be registered by the counting circuit. The same effect can be achieved in a slightly different way: by decreasing the height of all pulses by a constant small amount. Then the heights of the smallest pulses become negative. Those pulses are not registered. The MCA manufactured by the German company “PHYWE Systeme” has a software-controlled parameter “Offset”, which defines the mentioned decrease of pulse height. The increase of this parameter causes a shift of the pulse height spectrum to the left (the part of the spectrum that shifts into the region of negative pulses is eliminated). In the case of the mentioned MCA, at the highest gain, a unit of “Offset” corresponds to 40 channels. I. e., when Offset = 1, the spectrum shifts by 40 channels; when Offset = 2, the spectrum shifts by 80 channels, etc. Accordingly, when the “Offset” parameter is non-zero, Eq. 7.1 has to be modified as follows:

$$E = \frac{H + 40 \cdot \text{Offset}}{H_{\text{cal}} + 40 \cdot \text{Offset}} \cdot E_{\text{cal}}, \tag{7.2}$$

where $H$ and $H_{\text{cal}}$ are channel numbers corresponding to the "shifted" spectrum (it is assumed that the "Offset" parameter is the same both for the calibration spectrum and for the investigated spectrum).

During the measurements, the radioactive source and the detector must be inside a vacuum chamber. The vacuum is necessary in order to eliminate the systematic error in the measured energy caused by energy losses due to collisions of alpha particles with molecules of air.

## 7.2. Equipment and measurement procedure

For this experiment, a set of educational equipment manufactured by a German company "Phywe Systeme" is used. The main components of the equipment are the following:

1) alpha detector (semiconductor silicon surface barrier detector),
2) pre-amplifier for the alpha detector,
3) unsealed $^{241}$Am source for calibration of the alpha detector (activity 3.7 kBq),
4) sealed $^{226}$Ra source (activity 3 kBq; the source was manufactured in 2007, but the age of its radioactive material is not known),
5) vacuum container for nuclear physics experiments,
6) hand-held mano-/barometer,
7) two-stage diaphragm pump,
8) multichannel analyzer,
9) personal computer.

The view of the equipment is shown in Fig. 7.1. The radioactive source must be fastened to the adjustable source holder, which is at the right-hand side of the glass vessel (the "preparation side"). The detector is at the opposite end of the vessel. The multichannel analyzer has a built-in power supply for the detector.

During this experiment, two spectra must be measured: the calibration spectrum (using the unsealed $^{241}$Am source) and the investigated spectrum (using the investigated $^{226}$Ra source). The sequence of actions that must be done with each of the sources is the same; only the optimal distance between the source and the detector is different. The description of the measurement procedure is given below:

1. Remove three nuts on the right-hand cover of the glass vessel and remove this cover (together with the adjustable source holder).
2. Fasten the $^{241}$Am source to the adjustable source holder.
3. Place the vessel cover back to the glass vessel and screw the three nuts.
   **Warning:** The glass vessel must be handled very carefully in order to avoid cracking. At all times, the vessel must be in horizontal position, firmly placed on the table.

   **Note:** The $^{241}$Am source, which is used in this experiment for calibration of the detector, is also needed for Experiment No. 9 (in the latter experiment, the measurements with this source take about 40 min). If it is determined that the $^{241}$Am source is already used in another experiment, the current experiment must be started from measuring the $^{226}$Ra spectrum.

4. Switch on the hand-held mano-/barometer. It has two pressure sensors – internal and external – and consequently displays two values of pressure. The internal sensor measures the ambient pressure at all times. The external sensor is connected to the barometer with a cable, and to the vacuum chamber with a rubber tube. The arrow at the top of the LCD display of the manometer must be directed to the symbol "$P_{ext}$". If not, it must be placed beside this symbol using the button „▼". In this mode, the larger digits on the LCD show the pressure measured by the external sensor (i.e., the pressure inside the glass vessel), and the smaller digits show the ambient pressure. The unit of pressure is hectopascal (1 hPa = 100 Pa).

5. Close the ventilation screw on the left-hand side of the glass vessel. Switch on the pump and unscrew the black clamp that is on the rubber tube connecting the pressure sensor to the pump, as well as the orange clamp that is on the rubber tube connecting the pressure sensor to the vacuum chamber (see Fig. 7.1). Wait until the pressure in the glass vessel drops below 10 hPa. Then close the rubber tubes with the two clamps (first – the orange one, then the black one) and switch off the pump. ***Note***: After screwing the orange clamp, the pressure shown by the barometer will start growing rapidly, but one should keep in mind that this is not the pressure inside the vacuum chamber, which is sealed off by the orange clamp at this point.

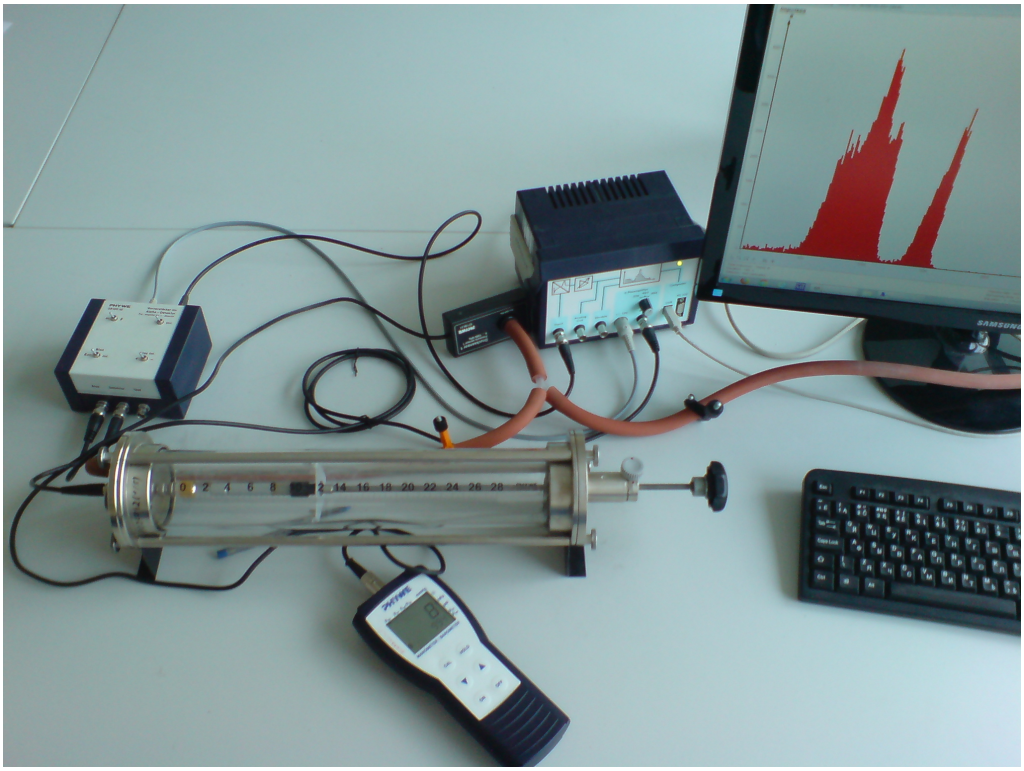

**Fig. 7.1.** General view of the measurement equipment

6. Check that the pre-amplifier switch "α/β" is in the position "α", the switch "Inv" is in the "Off" position (i. e., in the left position), and the switch "Bias" is in the position "Ext" (then the switch "Bias Int." may be in any position).

7. The switch "Bias" that is on the MCA must be in the position "–99 V". Switch on the MCA (the mains switch is on its back panel).

8. Start the program "Measure".

9. Prepare the program for the measurements, i. e.: **a)** click the menu command "Gauge/Multi Channel Analyser" (if the program then notifies about a failure to establish connection with the MCA, even though it is on and connected to the computer with a USB cable, then restart Windows), **b)** select the mode "Spectra recording" and click the button "Continue", **c)** in the list box "X-Data", select the item "Channel number" (this means that the quantity plotted on the X axis is the channel number), **d)** enter the number "10" in the text field "Interval width [channels]" and press the key "Enter" on the keyboard (then each bar of the graph will correspond to the sum of 10 adjacent channels), **e)** set the slider "Gain" to the rightmost position, **f)** enter the number "6" in the text box that is near the slider "Offset" and press the key "Enter" on the keyboard, **g)** if the check box "Start/Stop" is not checked, then click it, **h)** click the button "Reset". Then the program begins measuring the pulse height spectrum.

10. Decrease the distance between the source and the detector. ***Attention!*** The source holder must be pushed into the glass vessel carefully and slowly, so that the source housing does not touch the detector (otherwise the detector could be damaged).

11. The distance between the source and the detector determines the average counting rate (i.e., the average number of particles detected per unit time). The counting rate during the last two seconds is shown at the bottom of the main window of the program "Measure". This value can be used to adjust the distance between the source and the detector. The optimum distance between the source and the detector must be chosen on the basis of those two criteria:

a) *The total number of detected particles*: In the case of the calibration spectrum (with $^{241}$Am), it must be at least 20 000, and in the case of the investigated spectrum (with $^{226}$Ra), it must be at least 200 000 (the total number of detected particles is also shown, at the bottom left of the program window). The total number of detected particles must be as large as possible in order to improve the quality of the spectrum (because the relative standard error of the number of particles

in each channel is approximately equal to inverse square root of this number). It has been determined empirically that the mentioned optimal values of the total number of detected particles are sufficiently large for subsequent analysis. Thus, in order to ensure that the total measurement duration for each spectrum does not exceed $30\ \text{min} \approx 2 \times 10^3$ s, the average counting rate should exceed 20 000 / 2000 = 10 particles per second in the case of $^{241}$Am, and it should exceed 200 000 / 2000 = 100 particles per second in the case of $^{226}$Ra.

b) *The recovery time*: In the case of perfect equipment, the shape of the measured spectrum would depend only on the total number of detected particles (because it is the main factor that determines the statistical errors of the data). For example, the spectrum measured for 2 hours at the average counting rate of 500 particles / s would look practically the same as the spectrum measured for 20 hours at the average counting rate of 50 particles per second. However, a certain time must pass after each detected particle in order to ensure that the pulse of voltage caused by the next detected particle is not distorted (i.e., that it does not overlap with the previous pulse). This time is called the "recovery time" of the particle counting system. In order to minimize the mentioned distortions, the average time between two detected particles (i.e., the inverse average counting rate) must be much longer than the recovery time. In the case of the equipment used for this experiment, the mentioned distortions are acceptably small when the average counting rate is less than 200 particles per second. Thus, the distance between the detector and the source must be such that the average counting rate does not exceed 200 particles per second.

By merging both those requirements, the following condition for the "optimal" distance between the source and the detector is obtained: in the case of the calibration spectrum (with $^{241}$Am), this distance must be such that the counting rate is between 10 and 200 particles per second, and in the case of the investigated spectrum (with $^{226}$Ra), this distance must be such that the counting rate is between 100 and 200 particles per second.

***Note***: Since radioactive decay is a random process, the counting rate over the last 2 seconds (which is shown by the program), fluctuates in a relatively wide range, and it may occasionally be not inside the mentioned optimal interval. However, this is not a problem if the *majority* of the shown values belong to this interval.

12. Wait until the total number of detected particles exceeds the mentioned value (i.e., 20 000 in the case of the calibration spectrum, and 200 000 in the case of the investigated spectrum). In order to stop the measurement, click the check box "Start/Stop" (so that it becomes unchecked). Then click the button "Accept data". Then a new window with the final spectrum opens.

13. Check if the pressure inside the chamber has not become too high during the measurements. To do this, one has to unscrew the orange clamp. If the smallest pressure shown by the barometer after unscrewing the orange clamp is less than 100 hPa, this means that the increase of the pressure is not significant and the results of the measurements are not distorted by energy losses of alpha particles in the air that is between the radioactive source and the detector. ***Note***: After the orange clamp is unscrewed, the pressure inside the chamber will increase due to an influx of the air from the poorly sealed part of the vacuum system (between the two clamps), but the initial increase will be relatively small (less than 10 hPa), because the volume of the part of the system that is between the two clamps is much less than the volume of the vacuum chamber.

14. Save the graph. This is done by selecting the menu command "Measurement / Export data…". In the dialog window that pops up, check the boxes "Copy to clipboard" and "Export as metafile". Then create a Microsoft Word file and paste the graph into it. The graph may be additionally edited by inserting various labels into it.

15. Save the measurement data in table format for subsequent analysis. In order to do that, select the menu command "Measurement / Export data…" again, but now check the boxes "Save to file" and "Export as numbers". Then enter the complete file name. ***Note***: In the file, the data will be presented as two columns of numbers. The first column contains channel numbers and the second column contains corresponding numbers of pulses. Since during the measurements each ten adjacent channels were merged into a single channel, all channel numbers are multiples of 10.

16. Switch off the MCA.

17. In order to make it easier to open the vessel after ventilating it, loosen the three nuts on the preparation side (i.e., right-hand side) of the vessel.

18. Ventilate the vessel by unscrewing the ventilation screw on the left-hand side of the vessel.
19. Open the vessel (on the preparation side, i.e., the right-hand side).
20. Replace the radioactive source and repeat all measurements (Steps 3 to 20).
21. Remove the radioactive source and place it into its storage container. Cover the glass vessel.
22. Print the measurement data in table format. The tables must include only the channels that correspond to the observed peaks of the spectrum. The tables must be formatted so that they are clear. Each table must have a title and column headers; values of pressure must be included. Various programs may be used for formatting the tables (for example, "Microsoft Word" or "Microsoft Excel"). The list of printers in the "Print" dialog that pops up after selecting the menu command "File/Print" must contain the printer that is present in the laboratory. ***Notes***: 1) The printer that is currently used in the laboratory is not a network printer; instead it is connected to a computer that is connected to LAN. If the system can not establish connection with the printer, this probably means that the mentioned computer or the printer is not switched on. 2) If the mentioned computer and printer are switched on, but there still is an error message after an attempt to print, then open the folder "Computers Near Me" using "Windows Explorer", locate the computer with name "605-K3-2" and connect to it (user name is "Administrator", and the password field must be left empty). Then try printing again.
23. Write your name and surname on the printed sheets with measurement results. Show them to the laboratory supervisor for signing. Those sheets will have to be included in the final laboratory report for this experiment.

## 7.3. Analysis of measurement data

1. Determine the channel number $H_{\text{cal}}$ corresponding to the peak in the $^{241}$Am pulse height spectrum, and channel numbers corresponding to peaks of the $^{226}$Ra pulse height spectrum. If an isolated peak is visible at the left edge of the spectrum, it must be ignored, because it corresponds to "noise" pulses
2. Estimate errors of the obtained channel numbers. This estimate is based on the fact that the number of pulses corresponding to each channel is distributed according to the Poisson distribution. One of the properties of this distribution is that the standard deviation of a particle number is equal to the square root of the statistical average (in the case of a single measurement, this average is approximately equal to the result of this measurement). Hence, the square root of the number of pulses $n$ in channel $H$ is approximately equal to the standard deviation of this number $\sigma_n(H)$, and the 95 % confidence interval of the number of pulses is from $n(H) - 2\sigma_n(H) = n(H) - 2\sqrt{n(H)}$ to $n(H) + 2\sigma_n(H) = n(H) + 2\sqrt{n(H)}$. It follows that the confidence interval of the channel number corresponding to a given peak in the spectrum can be defined as the interval of $H$ values such that 95 % confidence intervals of the numbers of pulses ($n(H)$) in all channels of this interval overlap with the 95 % confidence interval of the maximum number of pulses corresponding to the same peak (see Fig. 7.2). In addition, this interval should be slightly expanded by adding two channels that are outside this interval (in the case of Fig. 7.2, those two channel numbers are 720 and 790). If the current peak overlaps with an adjacent peak, then only half of the width of the confidence interval must be measured. In such a case, the half-width of the confidence interval must be measured in the direction away from the interfering adjacent peak. For example, if the experimental spectrum is similar to the example shown in Fig. 7.3, then the half-width of the first peak must be measured to the left of the maximum, and the half-width of the third peak must be measured to the right of the maximum. The total width of the confidence interval is twice the measured half-width (i.e., it is assumed that the half-width measured in the other direction would be approximately equal to the current result, if there was no overlapping peak that interferes with the measurement).
3. Using formula (7.2), calculate energies of alpha particles emitted by $^{226}$Ra and their confidence intervals.
4. Calculate energy differences between the leftmost peak in the $^{226}$Ra spectrum and each of the other peaks of the same spectrum. Calculate confidence intervals of those energy differences. The uncertainty (standard error) of the difference of two energies must be calculated by applying the following general rule: the variance (i.e., squared standard error) of a difference or a sum of two random quantities is equal to the sum of variances of those two quantities.
5. Present results of Steps 3 and 4 of this section in the form of a table.

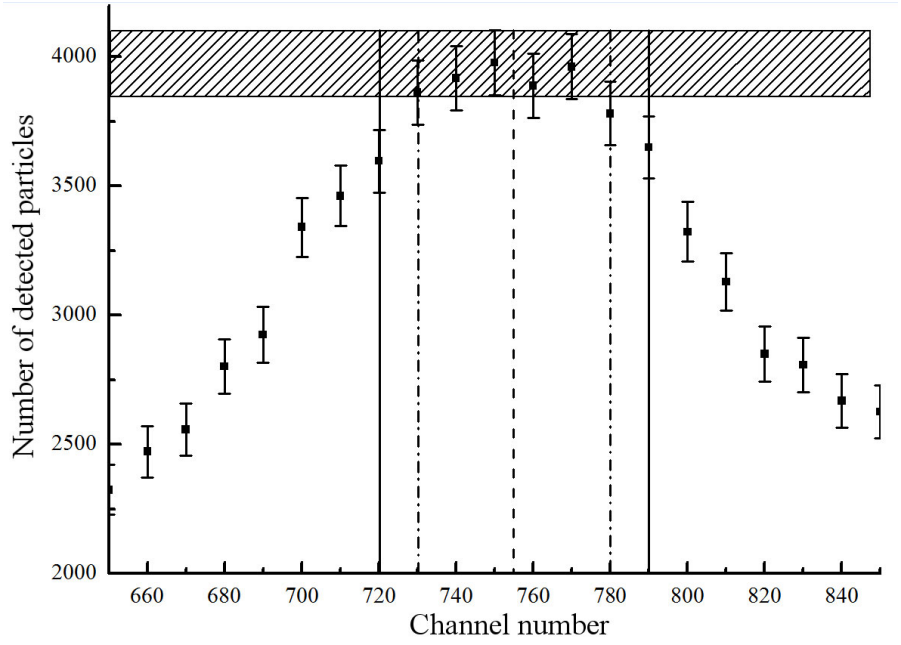


**Fig. 7.2.** Determination of the channel number $H_{max}$ corresponding to the maximum number of detected particles and its error. The vertical bars are the error indicating the 95 % confidence interval of each count (two standard deviations upwards from a point and two standard deviations downwards). The hatched area indicates the 95 % confidence interval of the maximum number of particles (in this example, the maximum number of particles corresponds to channel No. 750). This interval overlaps with 95 % confidence intervals of five additional points: two points to the left of the maximum and three points to the right of it (all those points are between the two vertical dash-dotted lines). After adding a point on each side, the 95 % confidence of $H_{max}$ is obtained. In this example, this interval is from $H = 720$ to $H = 790$ (see the two vertical solid lines), i.e., $H_{max} = 755 \pm 35$.

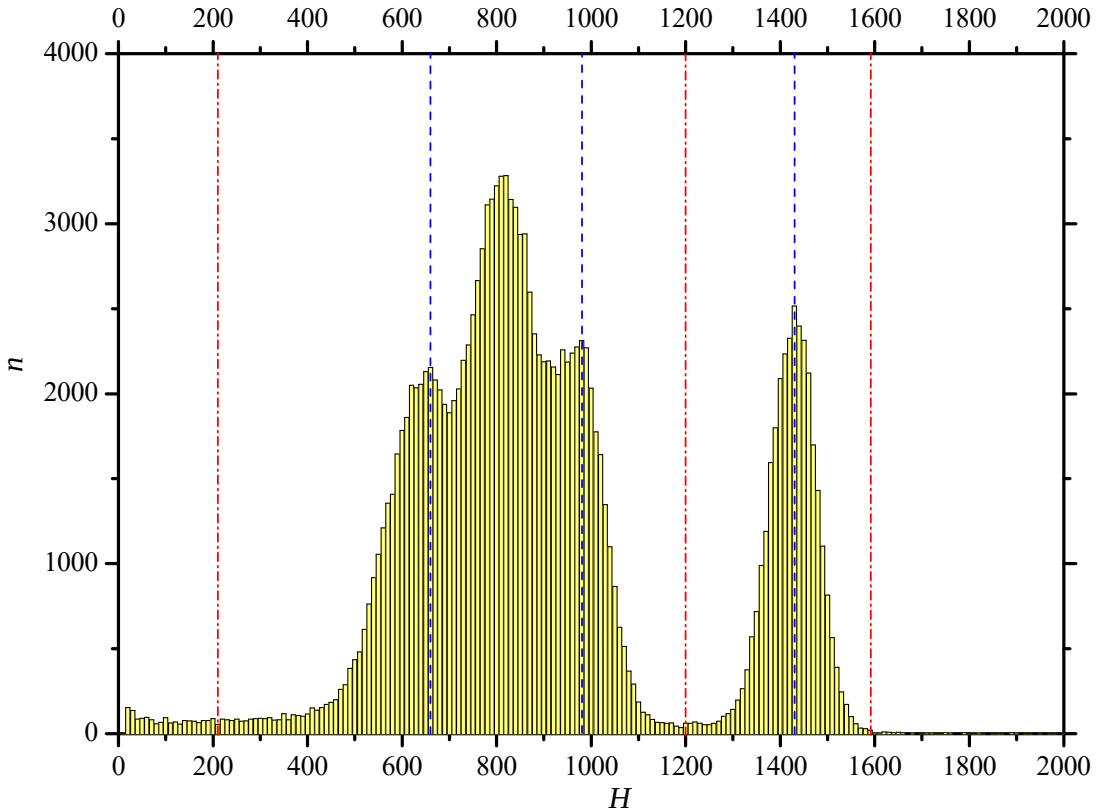


**Fig. 7.3**. An example of an experimental spectrum of the sealed $^{226}$Ra source. Blue dashed lines indicate the positions of maxima of peaks No. 1, 3 and 4 (the corresponding channel numbers are 660, 980, and 1430, respectively). Red dash-dotted lines indicate the endpoints of the summation intervals (the corresponding channel numbers are 210, 1200, and 1590).

6. Compare the obtained energy differences with the corresponding differences of the initial energies, which are given in Table 4.1e. On the basis of this comparison, identify the radioactive nuclides corresponding to each peak of the $^{226}$Ra spectrum. Ideally, the true energy differences should be inside the confidence intervals of the experimental energy differences (this would indicate that the nuclides were identified correctly).
7. Determine the integrals (areas) of the peaks of the $^{226}$Ra spectrum. The term "integral" will be further used to mean the total number of pulses (i.e., detected particles) corresponding to a particular peak, or to a group of overlapping peaks (it is not integral in the strict mathematical sense, because integration would involve multiplication by channel width, i.e., by 10). The endpoints of the summation interval must be determined using the following rules. The left endpoint of the summation interval of peak No. 4 corresponds to the channel whose number is equal to the average of the channel numbers corresponding to the maxima of peaks No. 3 and No. 4 (in the case of Fig. 7.3, this channel number is 1200), and the right endpoint corresponds to the leftmost channel where the number of pulses is less than 1/100 of the height of peak No. 4 (in the case of Fig. 7.3, this channel number is 1590). Since the remaining three peaks overlap with each other, it is impossible to determine their integrals separately. Instead, the *total* integral of those three peaks must be determined. The left endpoint of the corresponding summation interval is equal to half the channel number where the maximum of peak No. 1 is, after subtracting the correction equal to half of the leftward "shift" of the spectrum (see also end of Section 7.1), i.e., $40 \cdot \text{Offset} / 2 = 20 \cdot \text{Offset}$ (in the case of Fig. 7.3, $\text{Offset} = 6$, so that this endpoint is equal to $330 - 20 \cdot 6 = 210$), and the right endpoint coincides with the left endpoint of the summation integral of peak No. 4 (in the case of Fig. 7.3, this channel number is 1200). The results of this step of the analysis are the two values of the mentioned integrals: one of them corresponds to peak No. 4, and the other one corresponds to peaks No. 1 – 3.
8. Discuss the results. This discussion should include the conclusion regarding the validity of the mentioned assumption that all alpha particles lose the same amount of energy in the cover of the $^{226}$Ra source. In addition, the ratio of the two integrals calculated in the previous step should be used to determine if the nuclides of the decay chain of $^{226}$Ra are in radioactive equilibrium with each other. The theoretical value of the mentioned ratio in the case of radioactive equilibrium can be determined using the known number of alpha-emitting nuclides in the decay chain of $^{226}$Ra (see Table 4.1e) and the known fact that activities of all nuclides of this decay chain are equal at radioactive equilibrium.